# Qualitative failure of a multiconfiguration method in prolate spheroidal coordinates in calculating dissociative photoionization of H_{2}^{+}

Daniel J. Haxton, Keith V. Lawler, and C. William McCurdy

Phys. Rev. A **91**, 062502 — Published 9 June 2015

DOI: 10.1103/PhysRevA.91.062502

# Qualitative failure of a multiconfiguration method in prolate spheroidal coordinates in calculating dissociative photoionization of $H_2^+$

Daniel J. Haxton,[1] Keith V. Lawler,[2] and C. William McCurdy[1,3]

[1] *Chemical Sciences and Ultrafast X-ray Science Laboratory, Lawrence Berkeley National Laboratory, Berkeley CA 94720*
[2] *Department of Chemistry, University of Nevada-Las Vegas, Las Vegas NV 89154*
[3] *Departments of Applied Science and Chemistry, Davis CA 95616*

A formulation of multiconfiguration time-dependent Hartree-Fock (MCTDHF) with nuclear motion is tested by application to a three-body breakup problem, the dissociative photoionization cross section of the $H_2^+$ ion. The representation of the wave function in terms of a set of Slater determinants used for all nuclear geometries, with a prescribed parametric dependence upon the nuclear geometry such that the cusps follow the nuclei, times a complete basis expansion in the nuclear degrees of freedom shows promise as a method for treating nonadiabatic electronic and nuclear motion in molecules. However, the method used here for diatomics, in which the parametric dependence is prescribed through the choice of prolate spheroidal coordinates, produces qualitatively incorrect step-like behavior in the calculated cross section near onset. Modifications to the prolate spheroidal coordinate system that would improve this nonadiabatic diatomic MCTDHF representation are proposed.

PACS numbers: 31.15.-p, 33.80.Eh, 31.15.xv

## I. INTRODUCTION

Current and next generation experiments using ultrafast laser light demand *ab initio* methods for quantum electronic and nuclear molecular dynamics. There are many situations in which the coupling of nuclear and electronic motion results in strong deviations from the fixed-nuclei behavior. Notably, it was recently pointed out [1] that standard models of tunneling ionization must be modified to account for the effect of nuclear motion.

An effective all-purpose tool for calculating the response of a molecule to intense, short laser pulses must effectively describe both nonadiabatic nuclear motion and correlated many-electron quantum dynamics including ionization. The multiconfiguration time-dependent Hartree-Fock (MCTDHF) method [2–15] has received considerable attention for the electronic problem, and more than one group [10, 16, 17] have implemented MCTDHF methods including both electronic and nuclear motion. One of those [17, 18] is tested here by application to the simplest molecular three-body breakup problem, dissociative ionization of $H_2^+$.

The $H_2^+$ cation is the smallest molecule, and one that is relevant in environments ranging from interstellar chemistry [19, 20] to fusion reactors, and as such is well studied in the literature. It provides the one-electron archetype for fundamental processes such as dissociative recombination [20]. Due to its size, it is tractable to include nonadiabatic effects in calculating its dynamics [21, 22]. A comprehensive discussion of the interaction of $H_2^+$ with general laser fields is found in Ref. [23]. The two-body breakup, known as dissociative photoexcitation or photodissociation, has been studied experimentally [24–27] and theoretically [27–30], but our interest is in dissociative photoionization, the three-body breakup process. The three-body breakup has received much attention from theorists over the decades [31–35], and recently through the topic of differential cross sections [36] and interference effects [37–41]. Recent theoretical and experimental work on the system may be found in Refs. [42–49] and [50, 51], respectively. Even more recently, the interest in strong field and ultrafast physics has led to many experimental and numerical studies on coupled electronic and nyclear dynamics in this fundamental system [52–60].

The cross section derives from Fermi's golden rule, and is most directly pertinent to experiments performed with weak fields. The dissociative ionization and dissociative excitation cross sections were recently calculated using numerically exact methods within the nonrelativistic approximation and reported in Refs. [61] (including non adiabatic couplings) and [62] (in the Born-Oppenheimer approximation). The effect of the nonadiabatic coupling terms in the Hamiltonian was analyzed in Ref. [61]. Among other things, it was found that the doubly differential cross section (differential with respect to kinetic energy of the electron) is accurately calculated using a Born-Oppenheimer final state wave function, but is incorrect near onset when calculated with a Born-Oppenheimer initial state wave function.

To calculate a cross section using a time-dependent method we use weak pulses, as would the experiment. The code that we use [18] includes the ability to treat correlated nonadiabatic electronic and nuclear motion including ionization and dissociation with many electrons. It is formulated in prolate spheroidal coordinates, permitting an implementation of the exact nonrelativistic Hamiltonian for diatomic molecules [22]. We omit only Coriolis coupling terms, responsible for Lambda doubling, from this Hamiltonian.

The choice of prolate spheroidal coordinates here is not only a computationally expedient choice. On the contrary, within the present method [17], the choice of coor-

dinate system defines the nonadiabatic MCTDHF ansatz via the parametric dependence of orbitals upon nuclear geometry that it prescribes. This parametric dependence should be physical, e.g., orbitals on dissociating atoms should not change shape. The main conclusion of this work is that the prolate spheroidal coordinate system for diatomics must be modified, in order to improve the correlated representation of nuclear and electronic dynamics described in Ref. [17].

This is not the first application of a multiconfiguration method to fully nonadiabatic coupled electronic and nuclear dynamics. In Ref. [16] the $H_2^+$ ion was studied using MCTDH, that is, using an expansion in orbitals for the electron and nuclear degrees of freedom. A multi-electron version of this treatment is described in Ref. [10], and was applied the LiH molecule in Ref. [11]. The present method differs in that it uses orbitals for the electrons only, taking the full primitive basis expansion in the nuclear degree of freedom. In Ref. [11] it is written that our expansion is not explicitly time dependent in the nuclear part, but this statement is difficult to interpret because both methods compute a fully time dependent electronic and nuclear wave function.

The present approach [17, 18] uses a single set of orbitals defined in prolate spheroidal coordinates for all bond lengths, permitting a numerically compact representation of the multidimensional wave function. Prolate spheroidal coordinates are a choice that is arbitrary, except for the fact that they are nearly the easiest choice of bond-length-dependent coordinates to implement. In this method the electronic orbitals have a parametric dependence upon the bond length by way of the prolate coordinate system, denoted by a semicolon in the following expressions. The wave function is expanded in terms of a linear combination of Slater determinants at each value of the bond length, with each determinant comprised of time-dependent orbitals,

$$|\Psi(t)\rangle = \sum_{\kappa a} A_{\kappa a}(t)|\chi_\kappa(R)\rangle \times |\vec{n}_a(t;R)\rangle \qquad (1)$$

in which each determinant $\alpha$ is specified by the vector $\vec{n}_a$ and is defined by

$$|\vec{n}_a(t;R)\rangle = \mathscr{A}\left(|\phi_{n_{a1}}(t;R)\rangle \times ...|\phi_{n_{aN}}(t;R)\rangle\right) , \qquad (2)$$

where $\mathscr{A}$ is the antisymmetrizer. In contrast to the prescription here, Eq. 1, in the method of Refs. [10, 11] the wavefunction is expanded in terms $A_{\kappa a}(t)|\vec{N}_\kappa(t)\rangle\times|\vec{n}_a(t)\rangle$ using orbitals (determinants, cumulants, etc., $|\vec{N}_\kappa(t)\rangle$) for the nuclear motion. The present method using orbitals parametrically dependent upon nuclear geometry permits an accurate representation of the electron-nuclear cusp for all bond distances, but introduces cross terms in the electronic and nuclear kinetic energy because the total Hamiltonian is not separable in the four prolate spheroidal coordinates; they do not form an orthogonal coordinate system.

The time-dependent orbitals $|\phi_n(t)\rangle$ are spin-restricted, and expanded in an interpolating piecewise polynomial basis (a discrete variable representation [63–65]) using a spherical polar or prolate spheroidal grid as described in Ref. [17]. The grid is defined in the radial and polar directions and the primitive basis functions include factors of $e^{i\mathcal{M}\phi}/\sqrt{2\pi}$.

The cross sections are calculated within the time-dependent formalism [66, 67] and reported in Sec. II. Although they are generally correct over the full range of incident photon energies, they exhibit qualitatively incorrect step behavior at onset. This behavior is discussed in Sec. III. In Sec. IV, we describe the modification of prolate spheroidal coordinates that should improve this and other pathologies we have observed.

## II. $H_2^+$ PHOTOIONIZATION CROSS SECTIONS

Cross sections are calculated as described in Ref. [17]. We have previously reported a detailed test of the method for cross sections, which follows that of Ref. [67], in Ref. [68].

The dissociative photoionization cross section of $H_2^+$ is shown in Fig. 1. In this figure the present results are compared with an exact numerical treatment using the full grid in the electronic coordinates and bond length, and with the Born-Oppenheimer approximation at the equilibrium bond length of $2a_0$. As already mentioned, such exact results have previously been reported by us [61] and more recently in Ref. [62].

As in Ref. [61], we additionally compare the results of the Chase approximation [69] which entails a convolution of the Born-Oppenheimer result over the wave packets of the initial and final vibrational states,

$$\sigma^{CH}(E-E_0) = \int_0^E dE' \left| \int dR \sqrt{\sigma^{BO}\left(E'+\frac{1}{R}-E_0(R)\right)}\chi_0(R) f_l(k'',R)\right|^2 . \qquad (3)$$

In equation 3, $E_0$ is the vibrational ground state energy, $E_0(R)$ is the Born-Oppenheimer ground state energy as a function of the bond length, $\sigma^{CH}$ and $\sigma^{BO}$ are the Chase approximation to the cross section and the calculated Born-Oppenheimer cross sections, $\chi_0$ is the vibrational ground state, and $f_l$ is an energy-normalized continuum Coulomb wave function for nuclear motion on the repulsive $1/R$ potential of $H_2^{++}$, with $k''^2/2 = E - E'$. The cross sections are functions of photon energy. As can be seen here this approximation reproduces the exact result to very good accuracy, except at onset (the threshold for dissociative ionization, approximately 16.2eV, is substantially below onset, at approximately 25eV).

Cross sections for parallel and perpendicular polarization are shown in Fig. 1 as a function of the number of orbitals used to describe the single electron for all bond distances in prolate spheroidal coordinates. The initial state orbitals are necessarily all $\sigma_g$, because the

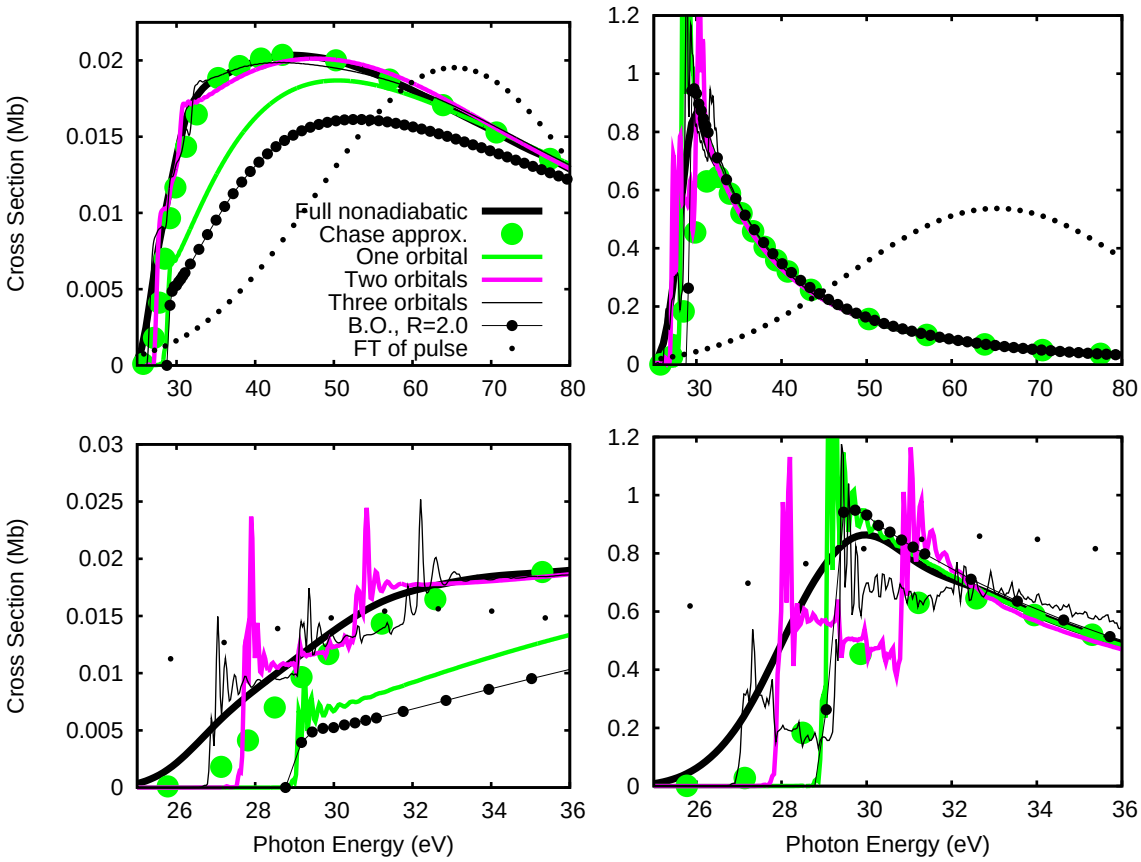


FIG. 1: (Color online) Cross sections for photoionization of $H_2^+$, including nonadiabatic nuclear motion in the bond length, calculated with one to four orbitals, compared to the Born-Oppenheimer result and to the Chase approximation. These are the results of four calculations, using two different laser pulses, one used to calculate the cross section up to 80eV and one for the onset region, for both parallel (left) and perpendicular (right) polarization.

masses are equal and Coriolis coupling terms were omitted. Coriolis coupling terms were tested and calculated to have an as-expectedly infinitesimal effect upon the dissociative photoionization cross section of the total angular momentum $J = 0$ ground state. The difference between the partial cross sections into the two components of the Lambda doublet for perpendicular polarization, and the effect of the coupling term upon the parallel polarization cross section, was on the order of machine precision or less. The Coriolis coupling terms are therefore neglected in the final results.

The present calculation depends upon the validity of a mean field approximation, and we find that we cannot use reasonable (about 1/100 femtosecond) mean field time steps without introducing large error into the solution. The off-diagonal terms in the kinetic energy for electrons and nuclei are probably making large contributions to the mean fields and the linear approximation to them that we use [17] is probably breaking down. All calculations except the one-orbital one have noise near onset that depends upon the mean-field parameters and that we were not able to easily remove. We have not been able to calculate results for four or more orbitals using reasonable mean field time steps.

The parallel ($\Sigma$) cross section is small. Over all energies plotted it is actually at a minimum with respect to bond distance at the equilibrium bond length of the cation ($R$=2a$_0$). Therefore the result with nuclear motion deviates significantly from and is higher than the Born-Oppenheimer result. In Fig. 1 we see that one orbital yields a result intermediate between the Born-Oppenheimer result at $R$=2.0a$_0$ and the exact nonadiabatic result, the latter of which is plotted as a black line in the figure. Except for the onset region, the calculation with two orbitals is converged to the exact result within visual accuracy.

In the Born-Oppenheimer approximation the cross section for perpendicular ($\Pi$) polarization is much larger than the $\Sigma$ cross section and relatively constant over the Frank-Condon region of the cation. Therefore, as shown in the bottom panel of Fig. 1, the full nonadiabatic result and the Born-Oppenheimer result at $R$=2a$_0$ are almost exactly identical. The multiconfiguration calculation reproduces the exact result with only one orbital. No straightforward argument for why this would be the case seems immediately obvious, and it would be interest-

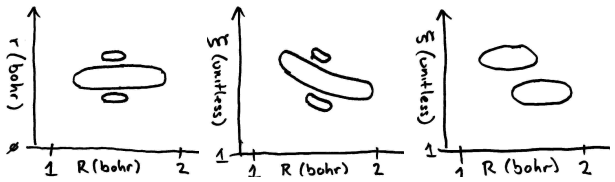


FIG. 2: Schematic of wave function density, $|\Psi(\vec{r},R)|^2$, integrated over angular coordinates, for an ionized wavepacket created by a short pulse, in spherical polar coordinates, left, and prolate spheroidal coordinates, middle. The hypothetical closest approximation to this wave packet using two orbitals in prolate coordinates is on the right.

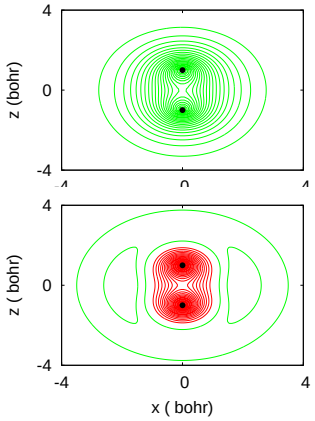


FIG. 3: (Color online) Initial natural orbitals (real-valued) $\phi(\vec{r};R)$, evaluated at $R$=2.0$a_0$, $y=0$, for two-orbital calculation.

ing to test the performance of the one-orbital calculation using different pulse envelopes.

The calculations show interesting behavior at onset, visible through the considerable numerical noise. The sharply peaked noise is dependent upon the nonphysical mean field parameters of the calculation – in other words, it is entirely numerical in origin. The salient discrepancy between the multiconfiguration results shown in Fig. 1 and the other results, numerical and physical, is that in the former there are a number of steps equaling the number of orbitals used in the calculations. Except for the step behavior at onset, the cross section seems to be converging to the exact result, which is close to the Chase approximation. We attempt a qualitative explanation of the step behavior in the following section, and in the conclusion we describe what would seem to be the solution.

## III. SPURIOUS STEP BEHAVIOR NEAR ONSET

We have observed the step behavior in the dissociative photoionization cross section at onset and now provide our best attempt at an explanation of it. Figure 2 shows a schematic. The essential contours of the density corresponding to an outgoing wave packet created by a short pulse are shown in the two coordinate systems, spherical polar (left) and prolate spheroidal (middle). Because the Hamiltonian is separable in the former, we expect wave fronts parallel with the grain of the coordinate system in the asymptotic region, and this is what we have drawn in the schematic at left. The left panel shows an outgoing electronic wavepacket not correlated with the nuclear degree of freedom $R$. The density at left is well represented as a product $P(R)\rho(r)$. In contrast, the density is not separable in prolate coordinates, middle, and any attempt to approximate it with few orbitals will compromise it, as in the right panel. The right panel shows a hypothetical best approximation to the middle panel using only two orbitals. We imagine that artificial nodes will be created and the fragmentation of smooth wave fronts seems a plausible explanation for the step behavior at onset.

We have not performed a falsifiable test of this hypothesis. We have plotted orbitals from the two-orbital calculation in search of this behavior and we show the results of that exercise in Figs. 3,4, and 5.

Ideally, the fragmentation behavior would be visible in the orbitals from the multiconfiguration calculation. However, the resolution of these orbitals that would be the best for this purpose is not obvious. We have choosen natural orbitals for Figs. 3,4, and 5 – natural orbitals for the electron, and for the bond distance, which together comprise the Schmidt decomposition of the wave function [17].

The natural orbitals diagonalize the reduced density matrices in the electronic ($\phi$) and nuclear coordinates ($\varphi$) of the prolate spheroidal coordinate system. They are not independent of this coordinate system, and different nonorthogonal coordinate systems will give different natural orbitals and occupancies. The two-orbital wave function expressed in terms of natural orbitals is

$$\Psi(\vec{r},R) = \lambda_1\phi_1(\vec{r};R)\varphi_1(R) + \lambda_2\phi_2(\vec{r};R)\varphi_2(R) \quad . \quad (4)$$

This expression is similar to a Schmidt decomposition but with the parametrically dependent coordinate.

Fig. 3, 4 and 5 show the electronic natural orbitals $\phi_1$ and $\phi_2$. Fig. 3 shows them before the pulse; these are the natural orbitals of the eigenfunction (stationary state). The node in $\phi_2$ is radial: this makes sense, due to the parametric dependence of the prolate spheroidal coordinate system for the electrons upon the bond length $R$. Because the size of the orbitals increases proportionally to the bond length, an orbital is required to describe "relaxation effects" in the radial degree of freedom. We refer to the well-known difference between the $2p$ Hartree-Fock orbitals in Neon and Neon cation as an example of the relaxation effect. The phenomenon observed here, similarly, is due to the difference in the fixed-nuclei Born-

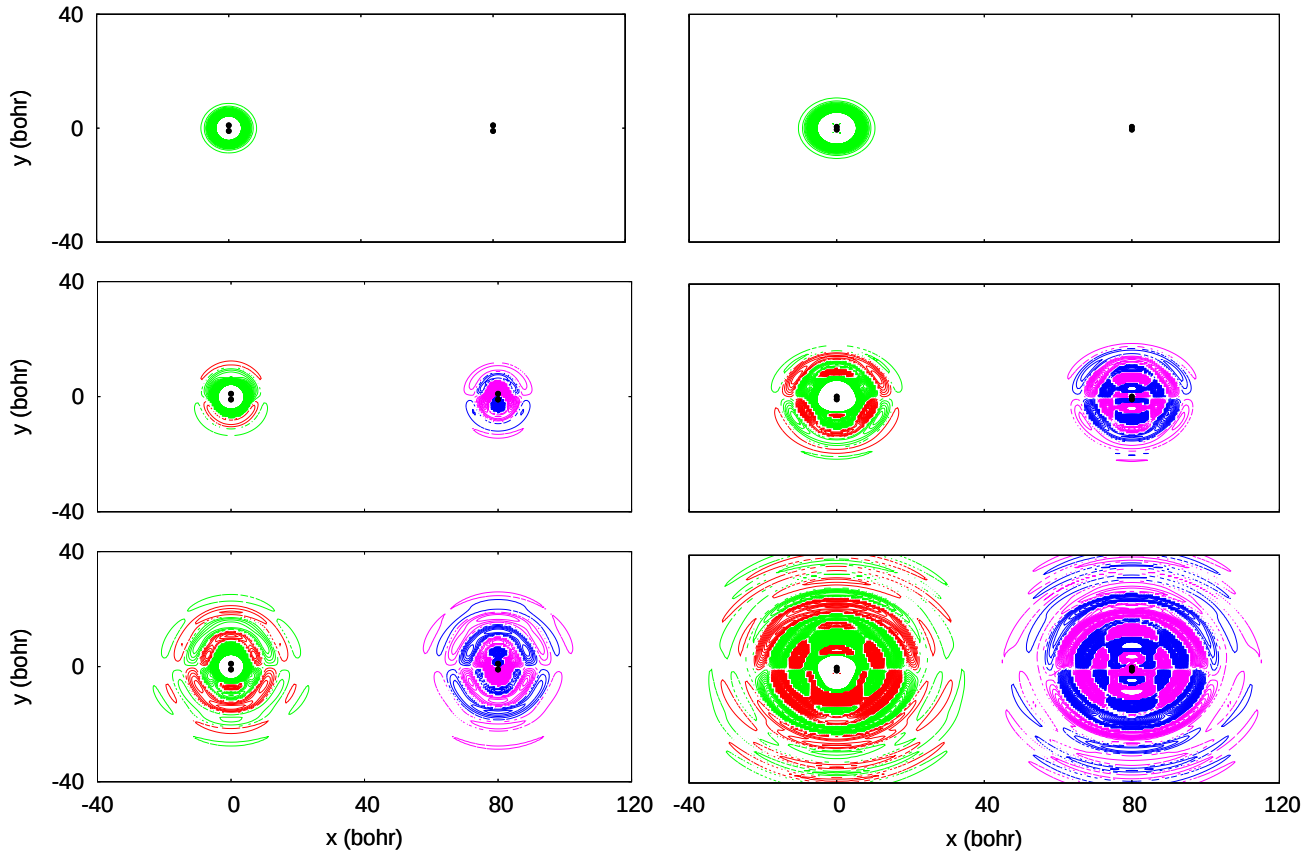


FIG. 4: (Color online) Natural orbitals $\phi(\vec{r};R)$ for 2-orbital propagation during the pulse, as the ionized flux moves outward, at (top to bottom) $t = 0$, 0.5, and 1.0fs after the start of the pulse, evaluated at $R$=2.0$a_0$, $y$=0. In each panel, the left image is the real part; the right, translated by 80 bohr, is the imaginary. The left three panels are the first natural orbital (occupancy approximately 96%) and the right are the second (4%)

Oppenheimer wave function for $H_2^+$ at the extrema of the Frank-Condon region. When the prolate spheroidal coordinates are changed to better describe the asymptotic region, as discussed in the conclusion, the nature of the node in the first correlating orbital may change, but the orbital will always belong to the totally symmetric irreducible representation.

Fig. 4 shows the natural orbitals during the pulse, at $t$ =0, 0.5, and 1.0fs. One can see flux moving outward. They are formally gauge-dependent and these have been calculated and plotted in the length gauge. (The multiconfiguration ansatz is gauge invariant; differences in results for different gauges betray basis set error in the primitive one-electron basis used to construct the orbitals.)

Fig. 5 shows the natural orbitals after the pulse, as the system is ringing down, at $t$ =0, 1.75, and 3.5fs after the end of the pulse. One can see the dominant wave number decreasing; higher mometa escape more quickly. We have attempted to identify some pattern in Figs. 4 and 5, by comparing these results to the natural orbitals from calculations with different ($\neq 2$) numbers of orbitals. No clear indication of the behavior depicted in the schematic in Fig. 2, going from the middle to the right panel, presented itself, and showing these results from calculations with different numbers (1, 3, 4, etc.) of orbitals seems to convey no more information. This issue must rest until a better method of analyzing the results is found, or until the behavior is ameliorated through the coordinate transformation described in the conclusion.

The analysis based on visual inspection of the natural orbitals presented here is lacking, but we consider the intuitive explanation of the step behavior at onset based on wave fronts to be compelling and perhaps there is evidence of it in our calculations, even in the figures here. In the next section, we discuss the solution to the step behavior problem, which should be clear at this point: the modification of the nonadiabatic MCTDHF ansatz, i.e., modifying the underlying coordinate system.

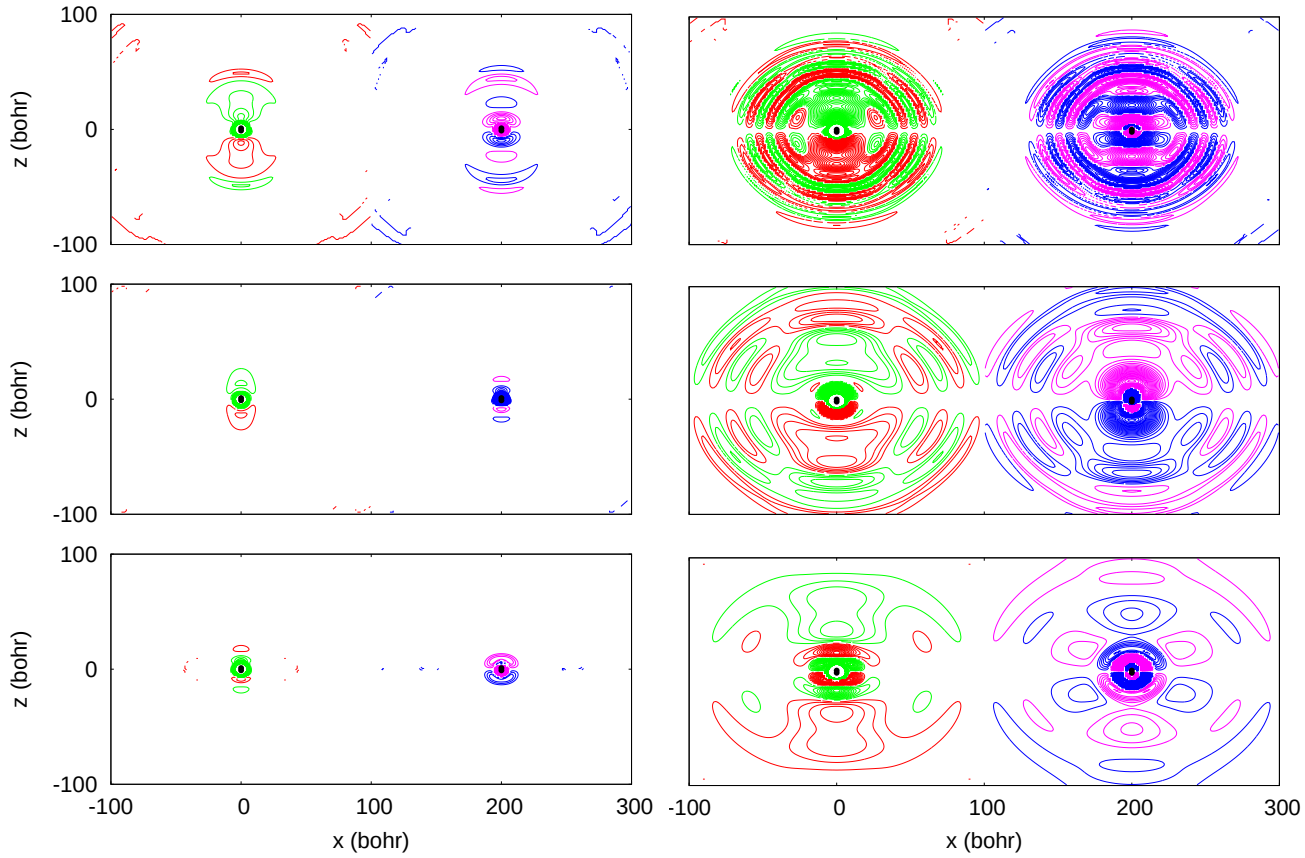


FIG. 5: (Color online) Natural orbitals $\phi(\vec{r}; 2.0)$ for 2-orbital propagation after the pulse, at $t$ =0, 1.75, and 3.75fs after the end of the pulse, as the wave function is ringing down, plotted in the same way as Fig. 4. At $R$ =2.0$a_0$, the wave function is absorbed via complex coordinate scaling starting at approximately $r = 80a_0$.

## IV. CONCLUSION

Although it produced results for bound vibronic ($J = 0$) states in good agreement with prior benchmark nonadiabatic calculations, the application to dissociative ionization has clearly strained this MCTDHF method for diatomic molecules [17, 18]. Although the large-scale behaviors of the $H_2^+$ dissociative photoionization cross sections calculated are accurate, for both parallel and perpendicular polarization the region near onset is calculated to contain a number of unphysical steps equal to the number of orbitals used in the calculation. Near onset, the total energy is the lowest possible for ionization, and the momentum is being shared most equally between electrons and nuclei. Therefore nonadiabatic effects are most important in this region [61, 70], and it is not unsurprising that this is the point of failure.

We have argued that because the prolate coordinates $\xi$ and $R$ are nonorthogonal, and therefore necessarily not aligned with the moments of inertia of the system, the outgoing wave describing the total breakup of the system that is the best approximation to the true solution with few orbitals will be fragmented. We did not elicit find this behavior in the wavefunctions that we calculated, but our analysis was visual and cursory and some evidence of it may lie in our data.

The method used here [17, 18] for nonadiabatic electronic and nuclear dynamics of diatomic molecules makes use of simplifications based on the prolate spheroidal coordinate system. These are among the easiest coordinates to program because the parametric dependence of the orbitals upon the nuclear geometry (the single coordinate $R$) is the simplest possible: their shape does not change, only their size. For a diatomic molecule, considering the triad of coordinates $(\eta, \xi, R)$, improving the coordinates means that a nonorthogonal coordinate transformation must be applied to these already-nonorthogonal coordinates. Keeping the orbitals orthogonal as a function of geometry will probably not be the most efficient ansatz for a diatomic nor polyatomic, so slow variable-discretization [71] or another method for operators differential in the nuclear coordinates will then need to be applied to matrix elements between Slater determinants at different geometries, and this issue presents a significant barrier. However, with the technology based

on biorthogonalization described in Ref. [17] and [68], and for small polyatomic vibrational motions excluding dissociation, this barrier may be easily crossed.

When the coordinate system that is parametrically dependent upon nuclear geometry is changed, the natural orbital occupations (which are not functions of nuclear geometry, the nuclear coordinates having been traced out) will change, and different coordinate systems will produce more efficient diatomic and polyatomic MCTDHF representations. We anticipate that an improved coordinate system will reduce or eliminate the step behavior at onset seen here. We also expect that it will reduce the number of orbitals that are required to converge both the cross section calculation for all energies, and the results for more-intense pulses for which Fermi's golden rule breaks down.

We conclude with two examples of coordinate systems that would be expected to improve the representation, based on the results and arguments we have presented in the prior three sections. It should be clear that we seek a coordinate system that, without loss of generality, approximately equals the spherical polar coordinate system at long range ($r >> R$). Here we will consider modifying only the $\xi$ prolate variable, defining a new variable $\zeta$ such that the coordinates are $(\zeta, \eta, \phi, R)$. The prolate coordinate $\eta$ is equal to $\cos\theta$ at long range. It is not clear what the absolutely-best $\zeta$ would be, but any of the following might suffice. Whereas the old coordinate is

$$\xi = \frac{\sqrt{x^2+y^2+\left(z-\frac{R}{2}\right)^2}+\sqrt{x^2+y^2+\left(z+\frac{R}{2}\right)^2}}{R} \quad , \tag{5}$$

and can be written more compactly

$$\xi = \frac{1}{R}\left(\sqrt{r^2+\frac{R^2}{4}-zR}+\sqrt{r^2+\frac{R^2}{4}+zR}\right) \quad , \tag{6}$$

two options for the new coordinate are $\zeta = \frac{R(\xi-1)}{2}$ and $\zeta = \frac{R}{2}\sqrt{\xi^2-1}$,

$$\zeta = \begin{cases} \xi = \frac{1}{2}\left(\sqrt{r^2+\frac{R^2}{4}-zR}+\sqrt{r^2+\frac{R^2}{4}+zR}-R\right) \\ \frac{1}{2}\left(\sqrt{2r^2-\frac{R^2}{2}+2\sqrt{\left(r^2+\frac{R^2}{4}\right)^2-R^2z^2}}\right) \end{cases} , \tag{7}$$

Either of these two choices for the new coordinate $\zeta$ replacing $\xi$ would make the coordinate system equal to spherical polar coordinates in the asymptotic region, and be amenable to a straightforward product grid. Any deviation from prolate spheroidal coordinates will necessitate separately calculating and storing the two-electron matrix elements for every $R$, but this is manageable due to the sparsity of these matrix elements. Which coordinate transformation gives the electronic and nuclear kinetic energy operator most easy to implement remains to be seen.

It is important to develop an all-purpose tool for solving the Schrödinger equation for chemical systems because current developments in ultrafast laser technology are beginning to open a new world of experiments manipulating and probing the structure of quantum matter. Our initial results here on a difficult problem – accurately computing the dissociative photoionization cross section – for the simplest system have pushed our implementation [18] to the breaking point. The method with nuclear motion is not useful presently due to the stability issues that precluded the appearance of results with more than three orbitals here. The cross sections calculated here are good enough to be useful, especially with prior knowledge of the pathology we have identified, and in fact were accurate with few orbitals over most of the domain of the cross section. Only at onset were they deficient. We have argued that the step behavior is the natural result of applying the present MCTDHF ansatz [17] with a coordinate system skewed relative to the moments of inertia of the system, as any set of nonorthogonal, Born-Oppenheimer-like coordinates defined relative to the nuclei will be, and presented several options for diatomic molecules that all should perform better than prolate spheroidal coordinates and that all are equivalent to spherical polar coordinates in the asymptotic region. Implementation of one or more of these coordinate transformations within the code used here [18] is a task for the future.

## V. ACKNOWLEDGEMENTS

We thank the National Energy Research Scientific Computing center (NERSC) for computational resources. Work performed at Lawrence Berkeley National Laboratory was supported by the US Department of Energy Office of Basic Energy Sciences, Division of Chemical Sciences Contract DE-AC02-05CH11231, and work at the University of California Davis was supported by US Department of Energy grant No. DESC0007182.

[1] O. I. Tolstikhin and L. B. Madsen, Phys. Rev. Lett. **111**, 153003 (2013), URL `http://link.aps.org/doi/10.1103/PhysRevLett.111.153003`.

[2] O. E. Alon, A. I. Streltsov, and L. S. Cederbaum, J. Chem. Phys. **127**, 154103 (2007).

[3] O. E. Alon, A. I. Streltsov, and L. S. Cederbaum, Phys. Rev. A **79**, 022503 (2009).

[4] M. Kitzler, J. Zanghellini, C. Jungreuthmayer, M. Smits, A. Scrinzi, and T. Brabec, Phys. Rev. A **70**, 041401 (2004).

[5] J. Caillat, J. Zanghellini, M. Kitzler, O. Koch, W. Kreuzer, and A. Scrinzi, Phys. Rev. A **71**, 012712

(2005).
[6] T. Kato and H. Kono, J. Chem. Phys. **128**, 184102 (2008).
[7] T. Kato and K. Yamanouchi, J. Chem. Phys. **131**, 164118 (2009).
[8] M. Nest, Phys. Rev. A **73**, 023613 (2006).
[9] M. Nest, R. Padmanaban, and P. Saalfrank, J. Chem. Phys. **126**, 214106 (2007).
[10] M. Nest, Chem. Phys. Letts. **472**, 171 (2009).
[11] I. S. Ulusoy and M. Nest, J. Chem. Phys. **136**, 054112 (2012).
[12] M. Nest, F. Remacle, and R. D. Levine, New J. Phys. **10**, 025019 (2008).
[13] D. Hochstuhl and M. Bonitz, J. Chem. Phys. **134**, 084106 (2011).
[14] R. P. Miranda, A. J. Fisher, L. Stella, and A. P. Horsfield, J. Chem. Phys. **134**, 244101 (2011).
[15] R. P. Miranda, A. J. Fisher, L. Stella, and A. P. Horsfield, J. Chem. Phys. **134**, 244102 (2011).
[16] C. Jhala and M. Lein, Phys. Rev. A **81**, 063421 (2010).
[17] D. J. Haxton, K. V. Lawler, and C. W. McCurdy, Phys. Rev. A **83**, 063416 (2011).
[18] D. J. Haxton, C. W. McCurdy, T. N. Rescigno, K. V. Lawler, B. Abeln, and X. Li, LBNL-AMO-MCTDHF, URL `https://commons.lbl.gov/display/csd/LBNL-AMO-MCTDHF`.
[19] A. Dalgarno, E. Herbst, S. Novick, and W. Klemperer, Astrophys. J. **183**, L131 (1973).
[20] T. Takagi, Physica Scripta **2002**, 52 (2002).
[21] I. Kawata, H. Kono, and Y. Fujimura, J. Chem. Phys. **110**, 11152 (1999).
[22] B. D. Esry and H. R. Sadeghpour, Phys. Rev. A **60**, 3604 (1999).
[23] A. Giusti-Suzor, F. H. Mies, L. F. DiMauro, E. Charron, and B. Yang, Journal of Physics B: Atomic, Molecular and Optical Physics **28**, 309 (1995), URL `http://stacks.iop.org/0953-4075/28/i=3/a=006`.
[24] F. von Busch and G. H. Dunn, Phys. Rev. A **5**, 1726 (1972).
[25] J.-B. Ozenne, D. Pham, and J. Durup, Chem. Phys. Lett. **17**, 422 (1972).
[26] N. P. F. B. van Asselt, J. G. Maas, and J. Los, Chem. Phys. **5**, 429 (1974).
[27] J.-B. Ozenne, J. Durup, R. W. Odom, C. Pernot, A. Tabche-Fouhaille, and M. Tadjeddine, Chem. Phys. **16**, 75 (1976).
[28] G. H. Dunn, Phys. Rev. **172**, 1 (1968).
[29] J. D. Argyros, J. Phys. B **7**, 2025 (1974).
[30] S. Saha, K. K. Datta, D. Basu, and A. K. Barau, J. Phys. B **13**, 3755 (1980).
[31] D. R. Bates, U. Opik, and G. Poots, Proc. Phys. Soc. A **66**, 1113 (1953).
[32] D. R. Bates and U. Opik, J. Phys. B **1**, 543 (1968).
[33] T. N. Rescigno and C. W. McCurdy, Phys. Rev. A **31**, 624 (1985).
[34] J. A. Richards and F. P. Larkins, J. Phys. B **19**, 1945 (1986).
[35] M. Morita and S. Yabushita, J. Comput. Chem. **29**, 2471 (2008).
[36] H. D. Cohen and U. Fano, Phys. Rev. **150**, 30 (1966).
[37] R. DellaPicca, P. D. Fainstein, M. L. Martiarena, and A. Dubois, Phys. Rev. A **75**, 032710 (2007).
[38] J. Fernandez, O. Fojon, A. Palacios, and F. Martin, Phys. Rev. Lett. **98**, 043005 (2007).
[39] R. DellaPicca, P. D. Fainstein, M. L. Martiarena, and A. Dubois, Phys. Rev. A **77**, 022702 (2008).
[40] J. Colgan, A. Huetz, T. J. Reddish, and M. S. Pindzola, J. Phys. B **41**, 085202 (2008).
[41] X. Guan, E. B. Secor, K. Bartschat, and B. I. Schneider, Phys. Rev. A **85**, 043419 (2012).
[42] H.-X. He, R.-F. Lu, P.-Y. Zhang, K.-L. Han, and G.-Z. He, Journal of Physics B: Atomic, Molecular and Optical Physics **45**, 085103 (2012), URL `http://stacks.iop.org/0953-4075/45/i=8/a=085103`.
[43] K. Doblhoff-Dier, K. I. Dimitriou, A. Staudte, and S. Gräfe, Phys. Rev. A **88**, 033411 (2013), URL `http://link.aps.org/doi/10.1103/PhysRevA.88.033411`.
[44] L. Yue and L. B. Madsen, Phys. Rev. A **88**, 063420 (2013), URL `http://link.aps.org/doi/10.1103/PhysRevA.88.063420`.
[45] H.-X. He, R.-F. Lu, P.-Y. Zhang, K.-L. Han, and G.-Z. He, The Journal of Chemical Physics **136**, 024311 (2012), URL `http://scitation.aip.org/content/aip/journal/jcp/136/2/10.1063/1.3676065`.
[46] A. Picón, A. Bahabad, H. C. Kapteyn, M. M. Murnane, and A. Becker, Phys. Rev. A **83**, 013414 (2011), URL `http://link.aps.org/doi/10.1103/PhysRevA.83.013414`.
[47] T.-Y. Xu and F. He, Phys. Rev. A **88**, 043426 (2013), URL `http://link.aps.org/doi/10.1103/PhysRevA.88.043426`.
[48] G. J. Halsz, A. Csehi, . Vibk, and L. S. Cederbaum, The Journal of Physical Chemistry A **118**, 11908 (2014), pMID: 24937768, http://dx.doi.org/10.1021/jp504889e, URL `http://dx.doi.org/10.1021/jp504889e`.
[49] H. Yao and G. Zhao, The Journal of Physical Chemistry A **118**, 9173 (2014), pMID: 24806756, http://dx.doi.org/10.1021/jp5030153, URL `http://dx.doi.org/10.1021/jp5030153`.
[50] K. Liu, P. Lan, C. Huang, Q. Zhang, and P. Lu, Phys. Rev. A **89**, 053423 (2014), URL `http://link.aps.org/doi/10.1103/PhysRevA.89.053423`.
[51] M. Odenweller, J. Lower, K. Pahl, M. Schütt, J. Wu, K. Cole, A. Vredenborg, L. P. Schmidt, N. Neumann, J. Titze, et al., Phys. Rev. A **89**, 013424 (2014), URL `http://link.aps.org/doi/10.1103/PhysRevA.89.013424`.
[52] K. Liu, W. Hong, Q. Zhang, and P. Lu, Optics Express **19**, 26359 (2011).
[53] K. Liu, Q. Zhang, and P. Lu, Phys. Rev. A **86**, 033410 (2012), URL `http://link.aps.org/doi/10.1103/PhysRevA.86.033410`.
[54] T. K. Kjeldsen, L. B. Madsen, and J. P. Hansen, Phys. Rev. A **74**, 035402 (2006), URL `http://link.aps.org/doi/10.1103/PhysRevA.74.035402`.
[55] A. K. Paul, S. Adhikari, D. Mukhopadhyay, G. J. Halasz, A. Vibok, R. Baer, and M. Baer, The Journal of Physical Chemistry A **113**, 7331 (2009), http://pubs.acs.org/doi/pdf/10.1021/jp811269g, URL `http://pubs.acs.org/doi/abs/10.1021/jp811269g`.
[56] V. S. Prabhudesai, U. Lev, A. Natan, B. D. Bruner, A. Diner, O. Heber, D. Strasser, D. Schwalm, I. Ben-Itzhak, J. J. Hua, et al., Phys. Rev. A **81**, 023401 (2010), URL `http://link.aps.org/doi/10.1103/PhysRevA.81.023401`.
[57] X. Guan, E. B. Secor, K. Bartschat, and B. I. Schneider, Phys. Rev. A **84**, 033420 (2011), URL `http://link.aps.org/doi/10.1103/PhysRevA.84.033420`.

[58] V. Roudnev and B. D. Esry, Phys. Rev. A **71**, 013411 (2005), URL http://link.aps.org/doi/10.1103/PhysRevA.71.013411.

[59] J. Zhao and Z. Zhao, Phys. Rev. A **78**, 053414 (2008), URL http://link.aps.org/doi/10.1103/PhysRevA.78.053414.

[60] B. Moser and G. N. Gibson, Phys. Rev. A **80**, 041402 (2009), URL http://link.aps.org/doi/10.1103/PhysRevA.80.041402.

[61] D. J. Haxton, Phys. Rev. A **88**, 013415 (2013).

[62] A. Igarashi, The European Physical Journal D **68**, 266 (2014), ISSN 1434-6060, URL http://dx.doi.org/10.1140/epjd/e2014-50268-2.

[63] A. S. Dickinson and P. R. Certain, J Chem Phys **49**, 4209 (1968).

[64] G. C. Corey and D. Lemoine, J Chem Phys **97**, 4115 (1992).

[65] J. C. Light, I. P. Hamilton, and J. V. Lill, J Chem Phys **82**, 1400 (1985).

[66] E. J. Heller, J. Chem. Phys. **62**, 1544 (1975).

[67] A. Jäckle and H.-D. Meyer, J. Chem. Phys. **105**, 6778 (1996).

[68] D. J. Haxton, K. V. Lawler, and C. W. McCurdy, Phys. Rev. A **86**, 013406 (2012).

[69] D. M. Chase, Phys. Rev. **104**, 838 (1956), URL http://link.aps.org/doi/10.1103/PhysRev.104.838.

[70] V. V. Serov and A. S. Kheifets, Phys. Rev. A **89**, 031402 (2014), URL http://link.aps.org/doi/10.1103/PhysRevA.89.031402.

[71] O. I. Tolstikhin, S. Watanabe, and M. Matsuzawa, Journal of Physics B: Atomic, Molecular and Optical Physics **29**, L389 (1996), URL http://stacks.iop.org/0953-4075/29/i=11/a=001.